DAFTAR PUSTAKA

[1] J. Gago and Y. Dala Ngapa, "PEMANFATAAN CANGKANG TELUR AYAM SEBAGAI MATERIAL DASAR DALAM SINTESIS HIDROKSIAPATIT DENGAN METODE PRESIPITASI BASAH," 2021.

[2] M. S. Hossain, M. N. Uddin, S. Sarkar, and S. Ahmed, "Crystallographic dependency of waste cow bone, hydroxyapatite, and β-tricalcium phosphate for biomedical application," *Journal of Saudi Chemical Society*, vol. 26, no. 6, Nov. 2022, doi: 10.1016/j.jscs.2022.101559.

[3] L. Anggresani, Y. N. Sari, and Rahmadevi, "Hydroxyapatite (HAp) From Tenggiri Fish Bones As Abrasive Material In Toothpaste Formula," *Jurnal Kimia Valensi*, vol. 7, no. 1, pp. 1–9, May 2021, doi: 10.15408/jkv.v7i1.19165.

[4] A. C. Ferro and M. Guedes, "Mechanochemical synthesis of hydroxyapatite using cuttlefish bone and chicken eggshell as calcium precursors," *Materials Science and Engineering C*, vol. 97, pp. 124–140, Apr. 2019, doi: 10.1016/j.msec.2018.11.083.

[5] C. H. Huang and M. Yoshimura, "Biocompatible hydroxyapatite ceramic coating on titanium alloys by electrochemical methods via Growing Integration Layers [GIL] strategy: A review," *Ceram Int*, vol. 49, no. 14, pp. 24532–24540, Jul. 2023, doi: 10.1016/j.ceramint.2022.12.248.

[6] M. M-Sam, M. Mayzan, and S. Rosli, "Properties of Calcium Hydroxyapatite Formed Using Waste Oyster Shell and Ammonium Dihydrogen Phosphate," *Sciences and Technology*, vol. 2, no. 2, pp. 229–237, 2022, doi: 10.30880/ekst.2022.02.02.024.

[7] B. Setyoko *et al.*, "Effect of carbonated hydroxyapatite synthesis from cuttlefish shells on orthodontic relapse prevention: in silico study," *Odonto : Dental Journal*, vol. 10, no. 1, p. 19, Jul. 2023, doi: 10.30659/odj.10.1.19-27.

[8] N. Rohmah and R. Ayu Kurniasih, "PENGARUH PERBEDAAN METODE EKSTRAKSI TERHADAP KARAKTERISTIK TEPUNG TULANG SOTONG (Sepia sp.) The Effect of Difference Extraction Methods on the Characteristics of Cuttlebone Powder (Sepia sp.)," 2022.

[9] S. Nurrahmi, N. Fuadi, and F. Yurdanianti, "Effect of Calcination mperature Variation on Hydroxyapatite of Cuttlefish Shell Waste (Sepia .)," *International License Gravitasi*, vol. 22, no. 1, pp. 31–34, 2023, doi: .22487/gravitasi.v22i1.16312.

[10] P. Vijayaraghavan *et al.*, “Preparation and antibacterial application of hydroxyapatite doped Silver nanoparticles derived from chicken bone,” *J King Saud Univ Sci*, vol. 34, no. 2, Feb. 2022, doi: 10.1016/j.jksus.2021.101749.

[11] “Synthesis of Calcium Phosphate from Boiler Egg Shells as Raw Material for Hydroxyapatite,” Galaxy Science, Nov. 2022. doi: 10.11594/nstp.2022.2718.

[12] N. Méndez-Lozano, M. Apátiga-Castro, K. M. Soto, A. Manzano-Ramírez, M. Zamora-Antuñano, and C. Gonzalez-Gutierrez, “Effect of temperature on crystallite size of hydroxyapatite powders obtained by wet precipitation process,” *Journal of Saudi Chemical Society*, vol. 26, no. 4, Jul. 2022, doi: 10.1016/j.jscs.2022.101513.

[13] J. Guo *et al.*, “Cold sintering: progress, challenges, and future opportunities,” *Annu Rev Mater Res*, vol. 49, pp. 275–295, 2019.

[14] D. O. Obada, E. T. Dauda, J. K. Abifarin, D. Dodoo-Arhin, and N. D. Bansod, “Mechanical properties of natural hydroxyapatite using low cold compaction pressure: Effect of sintering temperature,” *Mater Chem Phys*, vol. 239, Jan. 2020, doi: 10.1016/j.matchemphys.2019.122099.

[15] M. Khalid *et al.*, “Synthesis and characterizations of hydroxyapatite using precursor extracted from chicken egg shell waste,” *Biointerface Res Appl Chem*, vol. 12, no. 4, pp. 5663–5671, Aug. 2022, doi: 10.33263/BRIAC124.56635671.

[16] A. R. Razak, A. Stasya, Ruslan, and H. Ys, “Effect of Sintering Temperature on Hydroxyapatite Yield of Cuttlefish (Sepia sp.) Using the Wet Deposition Method,” 2023, pp. 286–294. doi: 10.2991/978-94-6463-228-6_32.

[17] Z. Miri *et al.*, “Review on the strategies to improve the mechanical strength of highly porous bone bioceramic scaffolds,” *Journal of the European Ceramic Society*, vol. 44, no. 1. Elsevier Ltd, pp. 23–42, Jan. 01, 2024. doi: 10.1016/j.jeurceramsoc.2023.09.003.

[18] P. M. Sivakumar, A. A. Yetisgin, E. Demir, S. B. Sahin, and S. Cetinel, “Polysaccharide-bioceramic composites for bone tissue engineering: A review,” *International Journal of Biological Macromolecules*, vol. 250. Elsevier B.V., Oct. 01, 2023. doi: 10.1016/j.ijbiomac.2023.126237.

[19] Kumar, S. Kargozar, F. Baino, and S. S. Han, “Additive Manufacturing ethods for Producing Hydroxyapatite and Hydroxyapatite-Based mposite Scaffolds: A Review,” *Frontiers in Materials*, vol. 6. Frontiers edia S.A., Dec. 17, 2019. doi: 10.3389/fmats.2019.00313.

[20] K. Fatma and J. Tripathy, “Bioceramic coatings for tissue engineering,” in *Advanced Ceramic Coatings for Emerging Applications*, Elsevier, 2023, pp. 291–309. doi: 10.1016/B978-0-323-99624-2.00002-4.

[21] K. W. Goh *et al.*, “Effect of pH on the properties of eggshell-derived hydroxyapatite bioceramic synthesized by wet chemical method assisted by microwave irradiation,” *Ceram Int*, vol. 47, no. 7, pp. 8879–8887, Apr. 2021, doi: 10.1016/j.ceramint.2020.12.009.

[22] E. Barua, A. B. Deoghare, P. Deb, S. Das Lala, and S. Chatterjee, “Effect of Pre-treatment and Calcination Process on Micro-Structural and Physico-Chemical Properties of Hydroxyapatite derived from Chicken Bone Bio-waste,” 2019. [Online]. Available: www.sciencedirect.comwww.materialstoday.com/proceedings2214-7853

[23] P. Arokiasamy *et al.*, “Synthesis methods of hydroxyapatite from natural sources: A review,” *Ceramics International*, vol. 48, no. 11. Elsevier Ltd, pp. 14959–14979, Jun. 01, 2022. doi: 10.1016/j.ceramint.2022.03.064.

[24] E.-S. Lee, P. Wadhwa, M.-K. Kim, H. B. Jiang, I.-W. Um, and Y.-M. Kim, “Organic matrix of enamel and dentin and developmental defects,” *Human Tooth and Developmental Dental Defects: Compositional and Genetic Implications*, vol. 27, p. 3, 2022.

[25] Z. Miri *et al.*, “Review on the strategies to improve the mechanical strength of highly porous bone bioceramic scaffolds,” *Journal of the European Ceramic Society*, vol. 44, no. 1. Elsevier Ltd, pp. 23–42, Jan. 01, 2024. doi: 10.1016/j.jeurceramsoc.2023.09.003.

[26] S. Panda, C. K. Biswas, and S. Paul, “A comprehensive review on the preparation and application of calcium hydroxyapatite: A special focus on atomic doping methods for bone tissue engineering,” *Ceramics International*, vol. 47, no. 20. Elsevier Ltd, pp. 28122–28144, Oct. 15, 2021. doi: 10.1016/j.ceramint.2021.07.100.

[27] N. A. A. Halim, M. Z. Hussein, and M. K. Kandar, “Nanomaterials-upconverted hydroxyapatite for bone tissue engineering and a platform for drug delivery,” *International Journal of Nanomedicine*, vol. 16. Dove Medical Press Ltd, pp. 6477–6496, 2021. doi: 10.2147/IJN.S298936.

[28] J. Xie, X. Sun, P. Li, T. Zhou, R. Jiang, and X. Wang, “The impact of ocean acidification on the eye, cuttlebone and behaviors of juvenile cuttlefish epiella inermis),” *Mar Pollut Bull*, vol. 190, May 2023, doi: .1016/j.marpolbul.2023.114831.

A. Jawad, *The Arabian Seas: Biodiversity, Environmental Challenges d Conservation Measures*. Springer International Publishing, 2021.

[Online]. Available: https://books.google.co.id/books?id=JLAmEAAAQBAJ

[30] S. Panda, C. K. Biswas, and S. Paul, “A comprehensive review on the preparation and application of calcium hydroxyapatite: A special focus on atomic doping methods for bone tissue engineering,” *Ceramics International*, vol. 47, no. 20. Elsevier Ltd, pp. 28122–28144, Oct. 15, 2021. doi: 10.1016/j.ceramint.2021.07.100.

[31] M. Safarzadeh, C. F. Chee, S. Ramesh, and M. N. A. Fauzi, “Effect of sintering temperature on the morphology, crystallinity and mechanical properties of carbonated hydroxyapatite (CHA),” *Ceram Int*, vol. 46, no. 17, pp. 26784–26789, Dec. 2020, doi: 10.1016/j.ceramint.2020.07.153.

[32] H. C. Ong, W. H. Chen, Y. Singh, Y. Y. Gan, C. Y. Chen, and P. L. Show, “A state-of-the-art review on thermochemical conversion of biomass for biofuel production: A TG-FTIR approach,” *Energy Conversion and Management*, vol. 209. Elsevier Ltd, Apr. 01, 2020. doi: 10.1016/j.enconman.2020.112634.

[33] A. Pambudi, M. Farid, and H. Nurdiansah, “Analisa Morfologi dan Spektroskopi Infra Merah Serat Bambu Betung (Dendrocalamus Asper) Hasil Proses Alkalisasi Sebagai Penguat Komposit Absorbsi Suara,” *Jurnal Teknik ITS*, vol. 6, no. 2, pp. F435–F440, 2017.

[34] J. Endro Suseno and K. S. Firdausi, “Rancang bangun spektroskopi FTIR (Fourier Transform Infrared) untuk penentuan kualitas susu sapi,” *Berkala Fisika*, vol. 11, no. 1, pp. 23–28, 2008.

[35] L. Hakim and D. M. Nawir, “Karakterisasi Struktur Material Pasir Bongkahan Galian Golongan C Dengan Menggunakan X-Ray Difraction (X-RD) Di Kota Palangkaraya,” 2019. [Online]. Available: http://e-journal.upr.ac.id/index.php/JMS

[36] S. Mustapha *et al.*, “Comparative study of crystallite size using Williamson-Hall and Debye-Scherrer plots for ZnO nanoparticles,” *Advances in Natural Sciences: Nanoscience and Nanotechnology*, vol. 10, no. 4, 2019, doi: 10.1088/2043-6254/ab52f7.

[37] P. Szterner and M. Biernat, “The Synthesis of Hydroxyapatite by Hydrothermal Process with Calcium Lactate Pentahydrate: The Effect of Reagent Concentrations, pH, Temperature, and Pressure,” *Bioinorg Chem pl*, vol. 2022, 2022, doi: 10.1155/2022/3481677.

A. Goldberg *et al.*, “The enhancement of hydroxyapatite thermal bility by Al doping,” *Journal of Materials Research and Technology*, l. 9, no. 1, pp. 76–88, Jan. 2020, doi: 10.1016/j.jmrt.2019.10.032.

[39] H. W. Fern and M. N. Salimi, “Hydroxyapatite nanoparticles produced by direct precipitation method: Optimization and characterization studies,” in *AIP Conference Proceedings*, American Institute of Physics Inc., May 2021. doi: 10.1063/5.0044252.

[40] S. Rahayu, D. W. Kurniawidi, and A. Gani, “PEMANFAATAN LIMBAH CANGKANG KERANG MUTIARA (PINCTADA MAXIMA) SEBAGAI SUMBER HIDROKSIAPATIT,” 2018.

[41] N. Selvia, K. Dahlan, and S. U. Dewi, “SINTESIS DAN KARAKTERISASI β-TRICALCIUM PHOSPHATE BERBASIS CANGKANG KERANG RANGA PADA VARIASI SUHU SINTERING,” 2012.

[42] S. Wisuda Sidauruk, D. Iriani, A. Diharmi, A. Anggraini, P. Studi Teknologi Hasil Perikanan, and F. Perikanan dan Kelautan, “VALORISASI CANGKANG KIJING AIR TAWAR (Pilsbryoconcha sp.) SEBAGAI SUMBER HIDROKSIAPATIT Valorisation of Fresh Water Mussel (Pilsbryoconcha sp.) Shells as Hydroxyapatite Source,” vol. 05, no. 02, pp. 85–92, 2022.

[43] N. Salsabila, V. Amalia, D. S. Rizka Fitriyani, and K. Kunci, “Seminar Nasional Kimia 2023 UIN Sunan Gunung Djati Bandung.”

[44] M. Sirait, K. Sinulingga, N. Siregar, and R. S. D. Siregar, “Synthesis of hydroxyapatite from limestone by using precipitation method,” in *Journal of Physics: Conference Series*, Institute of Physics Publishing, Mar. 2020. doi: 10.1088/1742-6596/1462/1/012058.

[45] Ö. Kesmez, “Preparation of anti-bacterial biocomposite nanofibers fabricated by electrospinning method,” *Journal of the Turkish Chemical Society, Section A: Chemistry*, vol. 7, no. 1, pp. 125–142, 2020, doi: 10.18596/jotcsa.590621.

[46] M. Lakrat, H. Jodati, E. M. Mejdoubi, and Z. Evis, “Synthesis and characterization of pure and Mg, Cu, Ag, and Sr doped calcium-deficient hydroxyapatite from brushite as precursor using the dissolution-precipitation method,” *Powder Technol*, vol. 413, Jan. 2023, doi: 10.1016/j.powtec.2022.118026.

[47] M. S. Hossain, M. N. Uddin, S. Sarkar, and S. Ahmed, “Crystallographic dependency of waste cow bone, hydroxyapatite, and β-tricalcium phosphate biomedical application,” *Journal of Saudi Chemical Society*, vol. 26, . 6, Nov. 2022, doi: 10.1016/j.jscs.2022.101559.

Sirait, K. Sinulingga, N. Siregar, and Y. F. Damanik, “Synthesis and aracterization of hydroxyapatite from broiler eggshell,” in *AIP*

Conference Proceedings, American Institute of Physics Inc., Mar. 2020. doi: 10.1063/5.0003043.

[49] M. Z. Ahmad Khiri *et al.*, "The effect of the pH values and sintering temperatures on the physical, structural and mechanical properties of nano hydroxyapatite derived from ark clam shells (Anadara granosa) prepared via the wet chemical precipitate method," *Ceramics - Silikaty*, vol. 63, no. 2, pp. 194–203, 2019, doi: 10.13168/cs.2019.0011.

[50] M. Z. A. Khiri *et al.*, "Crystallization behavior of low-cost biphasic hydroxyapatite/β-tricalcium phosphate ceramic at high sintering temperatures derived from high potential calcium waste sources," *Results Phys*, vol. 12, pp. 638–644, Mar. 2019, doi: 10.1016/j.rinp.2018.12.025.

[51] S. V. Harb *et al.*, "Hydroxyapatite and β-TCP modified PMMA-TiO2 and PMMA-ZrO2 coatings for bioactive corrosion protection of Ti6Al4V implants," *Materials Science and Engineering C*, vol. 116, Nov. 2020, doi: 10.1016/j.msec.2020.111149.

[52] N. Selvia, K. Dahlan, and S. U. Dewi, "SINTESIS DAN KARAKTERISASI β-TRICALCIUM PHOSPHATE BERBASIS CANGKANG KERANG RANGA PADA VARIASI SUHU SINTERING," 2012.

[53] P. Temperatur Sintering dan Komposisi Air dalam Suspensi terhadap Ukuran Kristal Hidroksiapatit Berbasis Tulang Sapi Aceh, I. Salsabila, dan Zulkarnain Jalil Jurusan Fisika, F. Matematika dan Ilmu PengetahuanAlam, and U. Jl Syekh Abdul Rauf, "The Effect of Sintering Temperature and Water Composition in Suspension to the Crystallite Size of Hydroxyapatite Based on Aceh's Bovine Bone," *J. Aceh Phys. Soc*, vol. 7, no. 3, pp. 157–161, 2018, [Online]. Available: http://www.jurnal.unsyiah.ac.id/JAcPS

[54] D. Nicolae Ungureanu, N. Angelescu, S. Elena Valentina, R. Mariana Ion, E. Valentina Stoian, and C. Zizi Rizescu, *Synthesis and characterization of hydroxyapatite nanopowders by chemical precipitation*. 2011. [Online]. Available: https://www.researchgate.net/publication/262322346

LAMPIRAN

Lampiran 1. Dokumentasi Penelitian

1. Preparasi Sampel

Tulang sotong dibersihkan

Tulang sotong dikeringkan (dibawah sinar matahari)

Tulang Sotong dihancurkan menjadi Serpihan kecil

Tulang sotong digiling

ulang sotong dihaluskan

Serbuk Tulang sotong Diayak

Bubuk tulang sotong dikalsinasi

Hasil Kalsinasi

2. Sintesis Hidroksiapatit

Bubuk kalsium Oksida (CaO)

Bubuk $(NH_4)_2HPO_4$

buatan Larutan 1

Pembuatan larutan 2

Titrasi Larutan 2 ke larutan 1

Stirrer larutan 1 dan larutan 2

Pengendapan 24 jam

Pencucian endapan

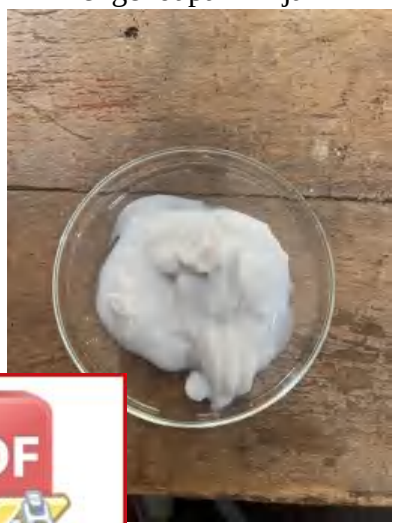

sil Pencucian

Pengeringan Endapan

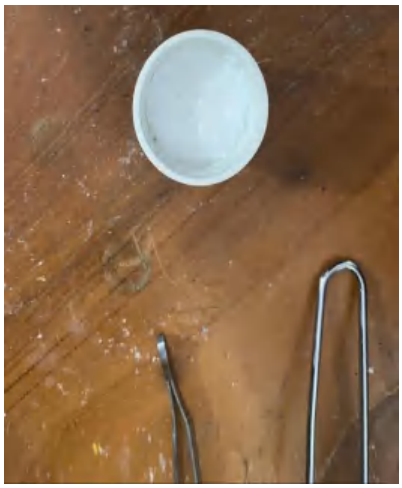

Setelah Pengeringan

Disintering pada suhu 700°C, 750°C, 800°C, dan 850°C selama 5 jam.

Hidroksiapatit Setelah disintering

Lampiran 2. Analisis Data

1. Analisis gugus fungsi menggunakan FTIR

a. Suhu 700°C

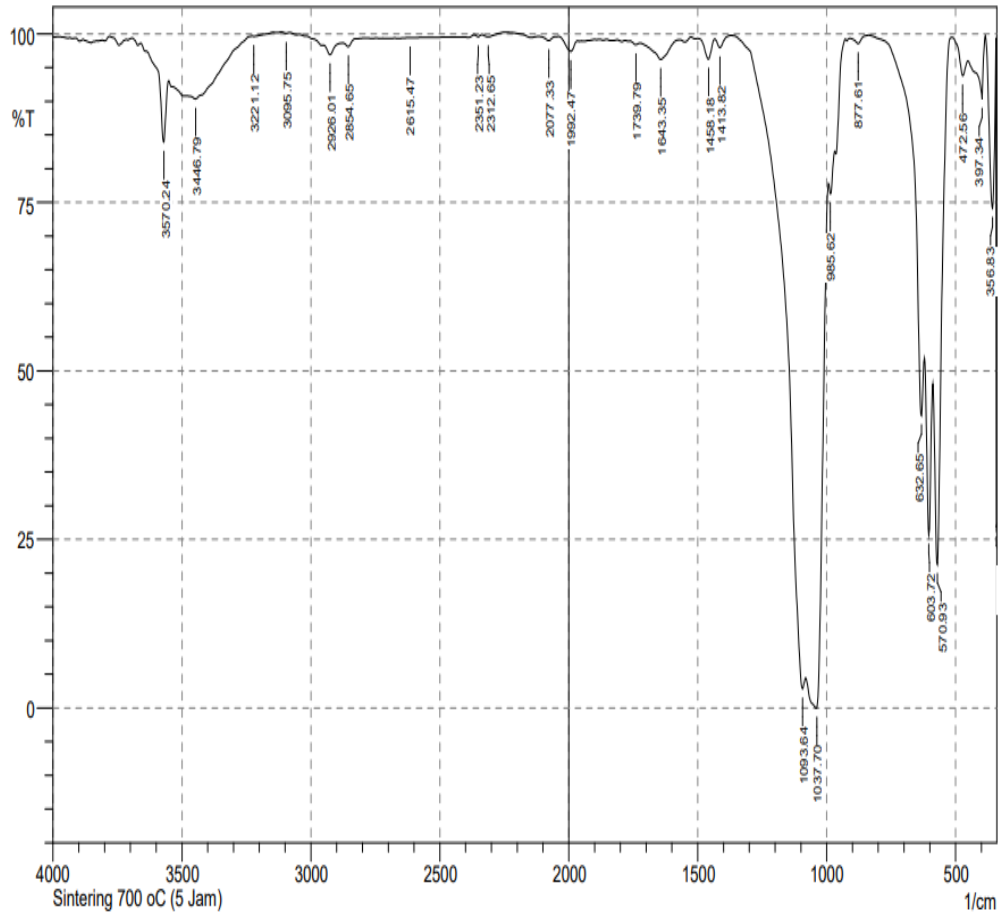

No.	Peak	Intensity	Corr. Intensity	Base (H)	Base (L)	Area	Corr. Area
1	341.4	26.782	36.63	343.33	339.47	2.188	0.559
2	356.83	74.137	20.995	383.83	345.26	2.863	2.218
3	397.34	90.333	8.709	451.34	385.76	1.628	1.016
4	472.56	93.816	3.288	513.07	453.27	0.897	0.294
5	570.93	21.327	38.929	588.29	514.99	18.191	7.851
6	603.72	25.674	23.552	619.15	590.22	12.912	3.997
7	632.65	43.419	11.055	837.11	621.08	13.881	1.179
8	877.61	98.568	0.985	910.4	837.11	0.242	0.108
9	985.62	76.272	2.735	991.41	970.19	2.21	0.185
10	1037.7	0	0.46	1045.42	1035.77	1544.933	1520.286
11	1093.64	2.861	5.462	1367.53	1082.07	75.135	2.842
12	1413.82	97.974	1.439	1433.11	1369.46	0.28	0.146
13	1458.18	96.274	3.004	1500.62	1433.11	0.575	0.365
14	1643.35	96.229	2.681	1724.36	1571.99	1.518	0.784
	1739.79	98.399	0.368	1762.94	1724.36	0.233	0.031
	1992.47	97.413	1.803	2036.83	1965.46	0.496	0.279

b. Suhu 750°C

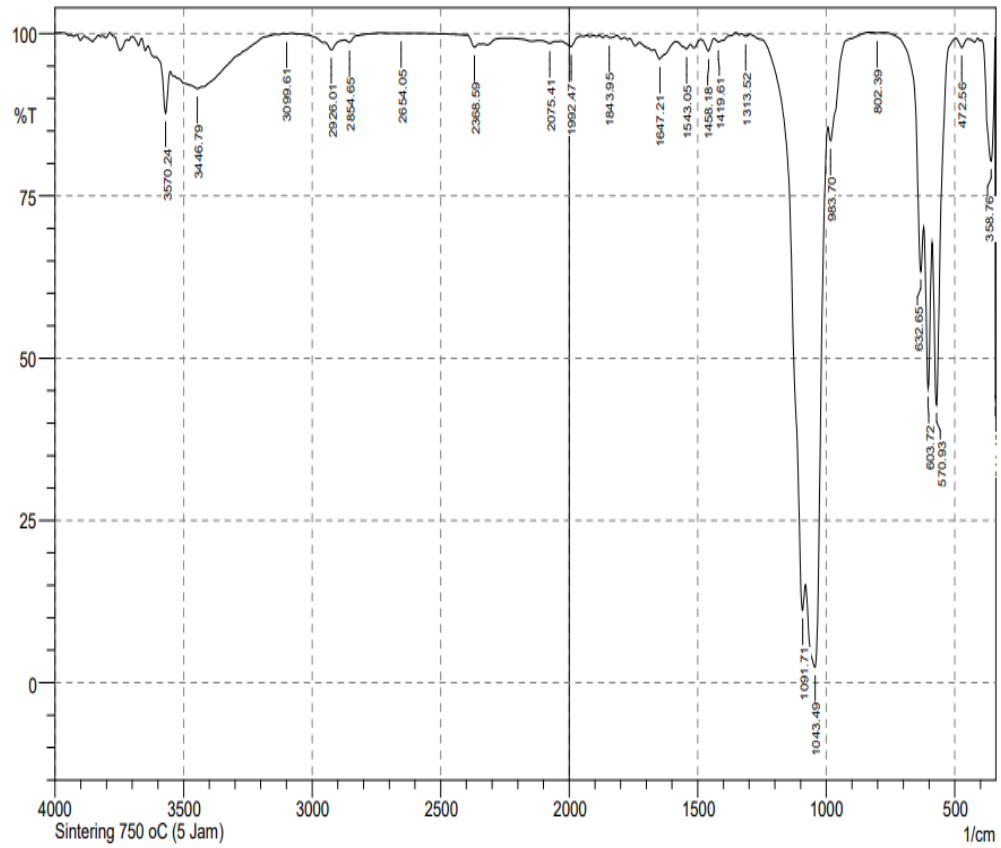

No.	Peak	Intensity	Corr. Intensity	Base (H)	Base (L)	Area	Corr. Area
1	341.4	43.871	28.109	343.33	339.47	1.368	0.349
2	358.76	80.387	15.607	395.41	345.26	2.773	2.076
3	472.56	97.849	1.398	495.71	449.41	0.28	0.128
4	570.93	42.83	29.876	586.36	497.63	10.256	4.066
5	603.72	45.294	23.421	619.15	588.29	7.735	2.693
6	632.65	63.389	9.063	775.38	621.08	5.836	0.682
7	802.39	100.101	0.093	833.25	777.31	-0.037	0.01
8	983.7	83.494	2.997	993.34	833.25	3.084	-2.241
9	1043.49	2.403	43.078	1080.14	995.27	71.04	34.671
10	1091.71	11.143	7.722	1298.09	1082.07	36.697	1.911
11	1313.52	99.593	0.374	1328.95	1300.02	0.033	0.028
12	1419.61	98.711	0.638	1436.97	1377.17	0.237	0.092
13	1458.18	97.349	1.828	1487.12	1436.97	0.362	0.181
14	1543.05	97.641	0.532	1556.55	1529.55	0.249	0.032
15	1647.21	96.12	1.729	1668.43	1587.42	0.984	0.325
16	1843.95	99.366	0.325	1857.45	1815.02	0.091	0.036

c. 800°C

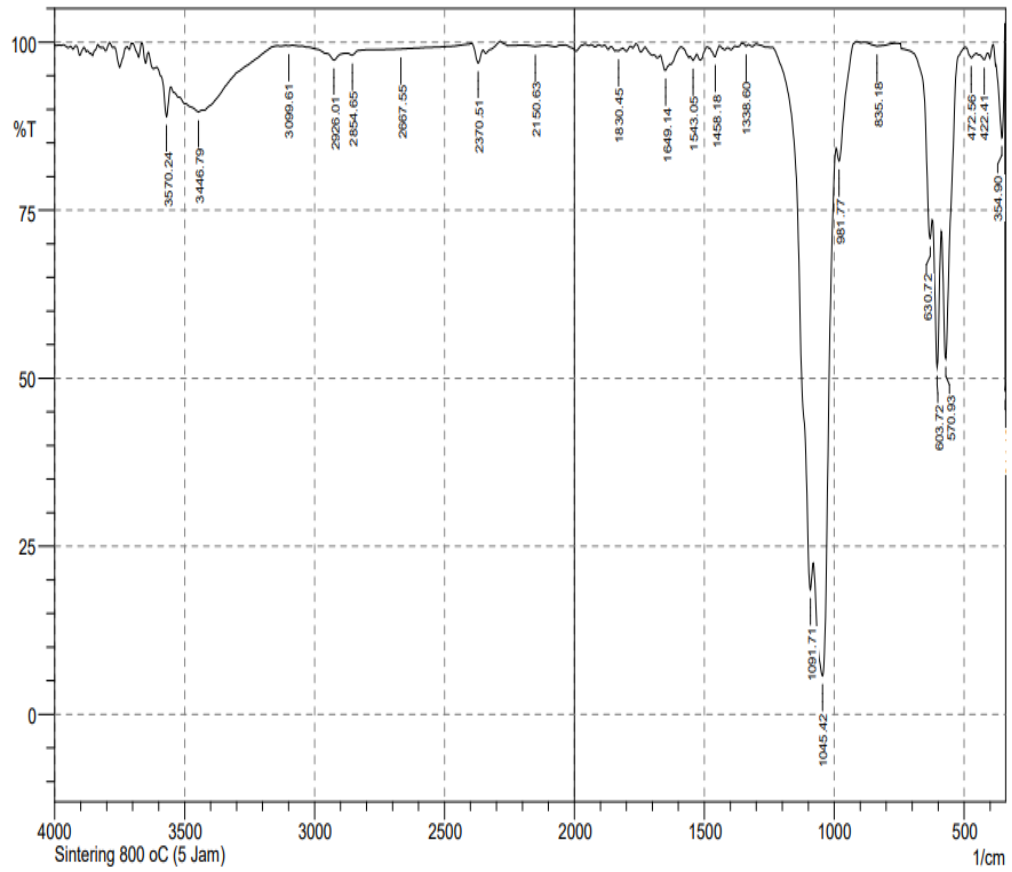

No.	Peak	Intensity	Corr. Intensity	Base (H)	Base (L)	Area	Corr. Area
1	341.4	48.03	27.994	343.33	339.47	1.208	0.329
2	354.9	85.771	11.439	376.12	345.26	1.311	0.903
3	422.41	97.401	0.85	441.7	408.91	0.311	0.056
4	472.56	97.681	1.06	495.71	453.27	0.32	0.095
5	570.93	52.94	23.454	586.36	497.63	8.77	3.302
6	603.72	51.644	20.925	621.08	588.29	6.899	2.332
7	630.72	70.797	4.444	738.74	623.01	4.369	0.277
8	835.18	99.382	0.546	885.33	761.88	0.187	0.141
9	981.77	82.317	3.915	991.41	916.19	2.763	0.355
10	1045.42	5.763	41.433	1080.14	993.34	56.9	26.516
11	1091.71	18.524	8.21	1255.66	1082.07	30.096	1.409
12	1338.6	99.414	0.302	1354.03	1328.95	0.043	0.015
13	1458.18	97.872	1.434	1479.4	1440.83	0.238	0.118
14	1543.05	97.27	0.733	1554.63	1529.55	0.26	0.041
15	1649.14	95.826	1.505	1668.43	1631.78	0.559	0.134
16	1830.45	98.694	0.184	1840.09	1815.02	0.129	0.01

d. Suhu 850°C

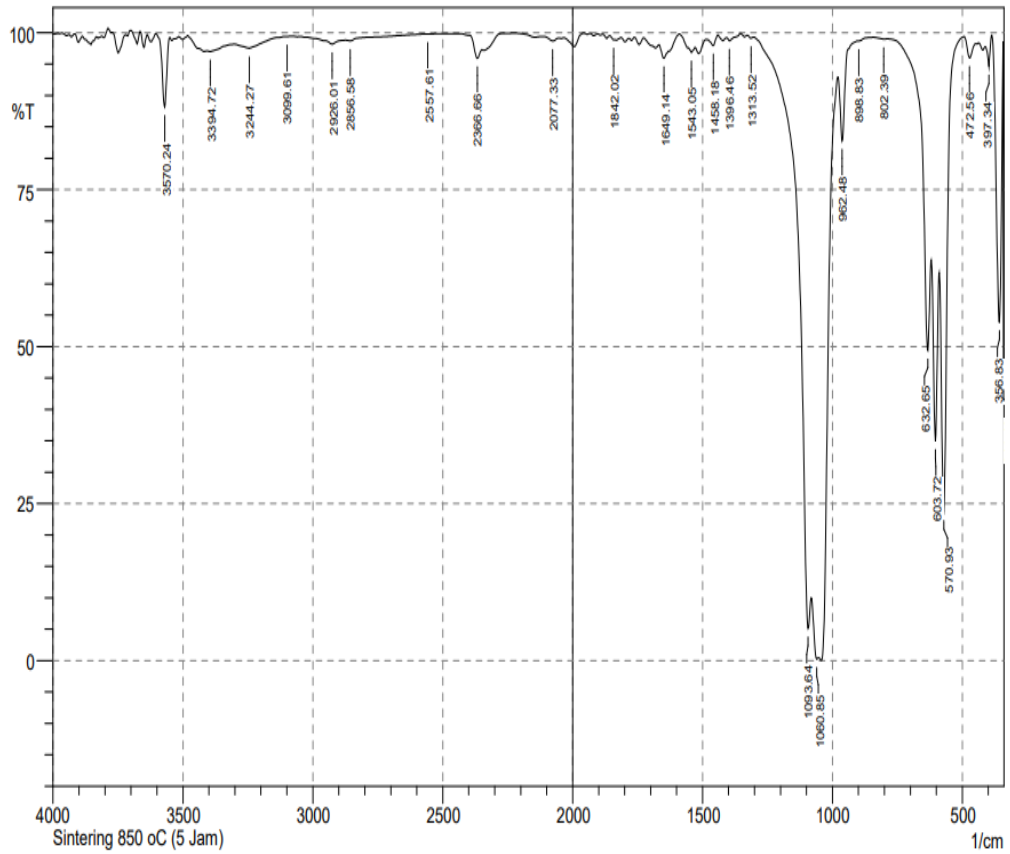

No.	Peak	Intensity	Corr. Intensity	Base (H)	Base (L)	Area	Corr. Area
1	341.4	44.473	28.214	343.33	339.47	1.316	0.354
2	356.83	53.886	38.359	385.76	345.26	5.553	4.476
3	397.34	94.602	4.284	412.77	387.69	0.334	0.188
4	472.56	95.962	2.872	493.78	449.41	0.489	0.258
5	570.93	23.657	45.03	588.29	493.78	14.18	7.337
6	603.72	34.989	27.502	619.15	590.22	9.385	3.475
7	632.65	49.373	16.566	786.96	621.08	10.108	1.735
8	802.39	98.985	0.096	842.89	786.96	0.221	0.011
9	898.83	98.687	0.02	900.76	842.89	0.237	-0.022
10	962.48	82.786	11.277	977.91	902.69	2.06	0.867
11	1060.85	0.274	2.355	1080.14	1055.06	45.613	3.499
12	1093.64	5.148	9.527	1301.95	1082.07	42.637	3.585
13	1313.52	99.129	0.271	1328.95	1303.88	0.076	0.014
14	1396.46	98.742	0.586	1408.04	1354.03	0.185	0.072
15	1458.18	97.947	1.338	1479.4	1440.83	0.234	0.107

1. **Analisis Sifat Struktur menggunakan *X-Ray Diffraction* (XRD) Suhu**

a. Suhu 700°C

*** Basic Data Process ***

Group : Standard
Data : asti#700#5

Strongest 3 peaks

no.	peak no.	2Theta (deg)	d (A)	I/I1	FWHM (deg)	Intensity (Counts)	Integrated Int (Counts)
1	8	31.7794	2.81351	100	0.78780	181	6741
2	9	32.7412	2.73302	63	0.48250	114	2853
3	4	25.7183	3.46117	39	0.44330	70	1744

Peak Data List

peak no.	2Theta (deg)	d (A)	I/I1	FWHM (deg)	Intensity (Counts)	Integrated Int (Counts)
1	16.8200	5.26680	4	0.40000	7	173
2	21.6800	4.09588	6	0.48000	11	281
3	22.7200	3.91069	5	0.36000	9	189
4	25.7183	3.46117	39	0.44330	70	1744
5	27.8066	3.20579	14	0.58670	26	711
6	28.8000	3.09743	14	0.44000	25	604
7	30.9400	2.88790	25	0.35000	45	927
8	31.7794	2.81351	100	0.78780	181	6741
9	32.7412	2.73302	63	0.48250	114	2853
10	34.0200	2.63316	23	0.69000	42	1419
11	35.3100	2.53986	6	0.54000	11	313
12	39.1000	2.30195	6	0.46000	11	266
13	39.6616	2.27064	24	0.45670	44	1046
14	41.8300	2.15781	7	0.54000	12	347
15	43.7450	2.06768	8	0.49000	15	427
16	45.2000	2.00445	4	0.28000	8	112
17	46.5691	1.94866	29	0.44830	53	1245
18	47.9666	1.89510	15	0.42670	27	651
19	49.3400	1.84551	34	0.40000	61	1228
20	50.3375	1.81125	14	0.40500	26	534
21	51.1316	1.78497	10	0.39670	18	334
22	51.9450	1.75892	10	0.35000	18	331
23	53.0505	1.72484	20	0.41100	37	779
24	55.7600	1.64727	6	0.44000	10	238
25	56.9200	1.61643	3	0.40000	6	176
26	58.0500	1.58762	3	0.18000	5	95
27	59.9200	1.54247	6	0.80000	10	363
28	61.4900	1.50679	7	0.38000	13	283
29	62.9050	1.47626	8	0.47000	15	387
30	63.9350	1.45494	14	0.47000	26	647
31	64.8500	1.43660	8	0.70000	14	495
32	66.2500	1.40960	5	0.30000	9	174
33	71.4300	1.31956	4	0.46000	8	263
34	72.2600	1.30644	3	0.16000	5	72
35	73.7500	1.28368	4	0.42000	8	204

*** Basic Data Process ***

Data Infomation

Group	:	Standard
Data	:	asti#700#5
Sample Nmae	:	powder
Comment	:	
Date & Time	:	01-12-24 07:18:48

Measurement Condition

X-ray tube		
target	:	Cu
voltage	:	40.0 (kV)
current	:	30.0 (mA)
Slits		
Auto Slit	:	not Used
divergence slit	:	1.00000 (deg)
scatter slit	:	1.00000 (deg)
receiving slit	:	0.30000(mm)
Scanning		

b. Suhu 750°C

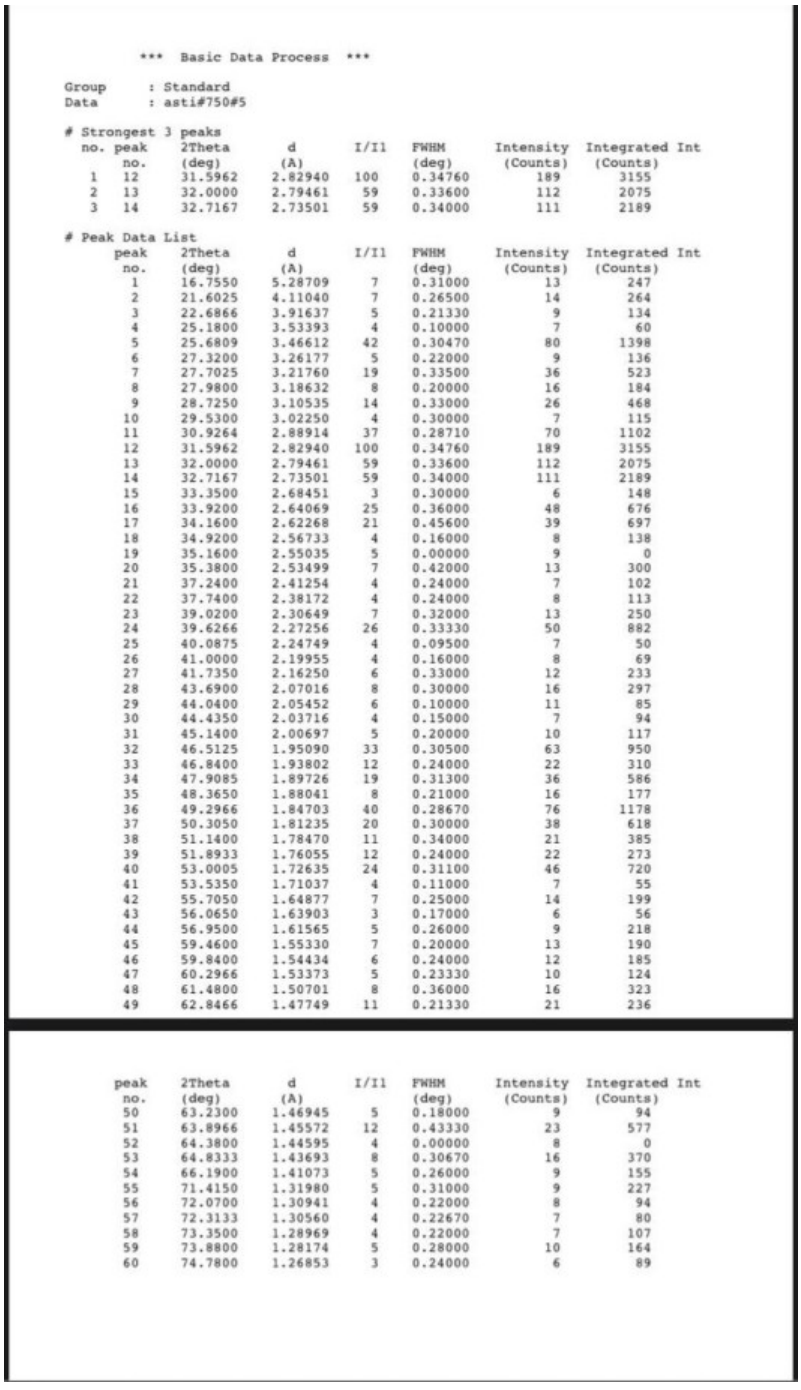

*** Basic Data Process ***

Group : Standard
Data : asti#750#5

Strongest 3 peaks

no. peak no.	2Theta (deg)	d (A)	I/I1	FWHM (deg)	Intensity (Counts)	Integrated Int (Counts)
1 12	31.5962	2.82940	100	0.34760	189	3155
2 13	32.0000	2.79461	59	0.33600	112	2075
3 14	32.7167	2.73501	59	0.34000	111	2189

Peak Data List

peak no.	2Theta (deg)	d (A)	I/I1	FWHM (deg)	Intensity (Counts)	Integrated Int (Counts)
1	16.7550	5.28709	7	0.31000	13	247
2	21.6025	4.11040	7	0.26500	14	264
3	22.6866	3.91637	5	0.21330	9	134
4	25.1800	3.53393	4	0.10000	7	60
5	25.6809	3.46612	42	0.30470	80	1398
6	27.3200	3.26177	5	0.22000	9	136
7	27.7025	3.21760	19	0.33500	36	523
8	27.9800	3.18632	8	0.20000	16	184
9	28.7250	3.10535	14	0.33000	26	468
10	29.5300	3.02250	4	0.30000	7	115
11	30.9264	2.88914	37	0.28710	70	1102
12	31.5962	2.82940	100	0.34760	189	3155
13	32.0000	2.79461	59	0.33600	112	2075
14	32.7167	2.73501	59	0.34000	111	2189
15	33.3500	2.68451	3	0.30000	6	148
16	33.9200	2.64069	25	0.36000	48	676
17	34.1600	2.62268	21	0.45600	39	697
18	34.9200	2.56733	4	0.16000	8	138
19	35.1600	2.55035	5	0.00000	9	0
20	35.3800	2.53499	7	0.42000	13	300
21	37.2400	2.41254	4	0.24000	7	102
22	37.7400	2.38172	4	0.24000	8	113
23	39.0200	2.30649	7	0.32000	13	250
24	39.6266	2.27256	26	0.33330	50	882
25	40.0875	2.24749	4	0.09500	7	50
26	41.0000	2.19955	4	0.16000	8	69
27	41.7350	2.16250	6	0.33000	12	233
28	43.6900	2.07016	8	0.30000	16	297
29	44.0400	2.05452	6	0.10000	11	85
30	44.4350	2.03716	4	0.15000	7	94
31	45.1400	2.00697	5	0.20000	10	117
32	46.5125	1.95090	33	0.30500	63	950
33	46.8400	1.93802	12	0.24000	22	310
34	47.9085	1.89726	19	0.31300	36	586
35	48.3650	1.88041	8	0.21000	16	177
36	49.2966	1.84703	40	0.28670	76	1178
37	50.3050	1.81235	20	0.30000	38	618
38	51.1400	1.78470	11	0.34000	21	385
39	51.8933	1.76055	12	0.24000	22	273
40	53.0005	1.72635	24	0.31100	46	720
41	53.5350	1.71037	4	0.11000	7	55
42	55.7050	1.64877	7	0.25000	14	199
43	56.0650	1.63903	3	0.17000	6	56
44	56.9500	1.61565	5	0.26000	9	218
45	59.4600	1.55330	7	0.20000	13	190
46	59.8400	1.54434	6	0.24000	12	185
47	60.2966	1.53373	5	0.23330	10	124
48	61.4800	1.50701	8	0.36000	16	323
49	62.8466	1.47749	11	0.21330	21	236

peak no.	2Theta (deg)	d (A)	I/I1	FWHM (deg)	Intensity (Counts)	Integrated Int (Counts)
50	63.2300	1.46945	5	0.18000	9	94
51	63.8966	1.45572	12	0.43330	23	577
52	64.3800	1.44595	4	0.00000	8	0
53	64.8333	1.43693	8	0.30670	16	370
54	66.1900	1.41073	5	0.26000	9	155
55	71.4150	1.31980	5	0.31000	9	227
56	72.0700	1.30941	4	0.22000	8	94
57	72.3133	1.30560	4	0.22670	7	80
58	73.3500	1.28969	4	0.22000	7	107
59	73.8800	1.28174	5	0.28000	10	164
60	74.7800	1.26853	3	0.24000	6	89

c. Suhu 800°C

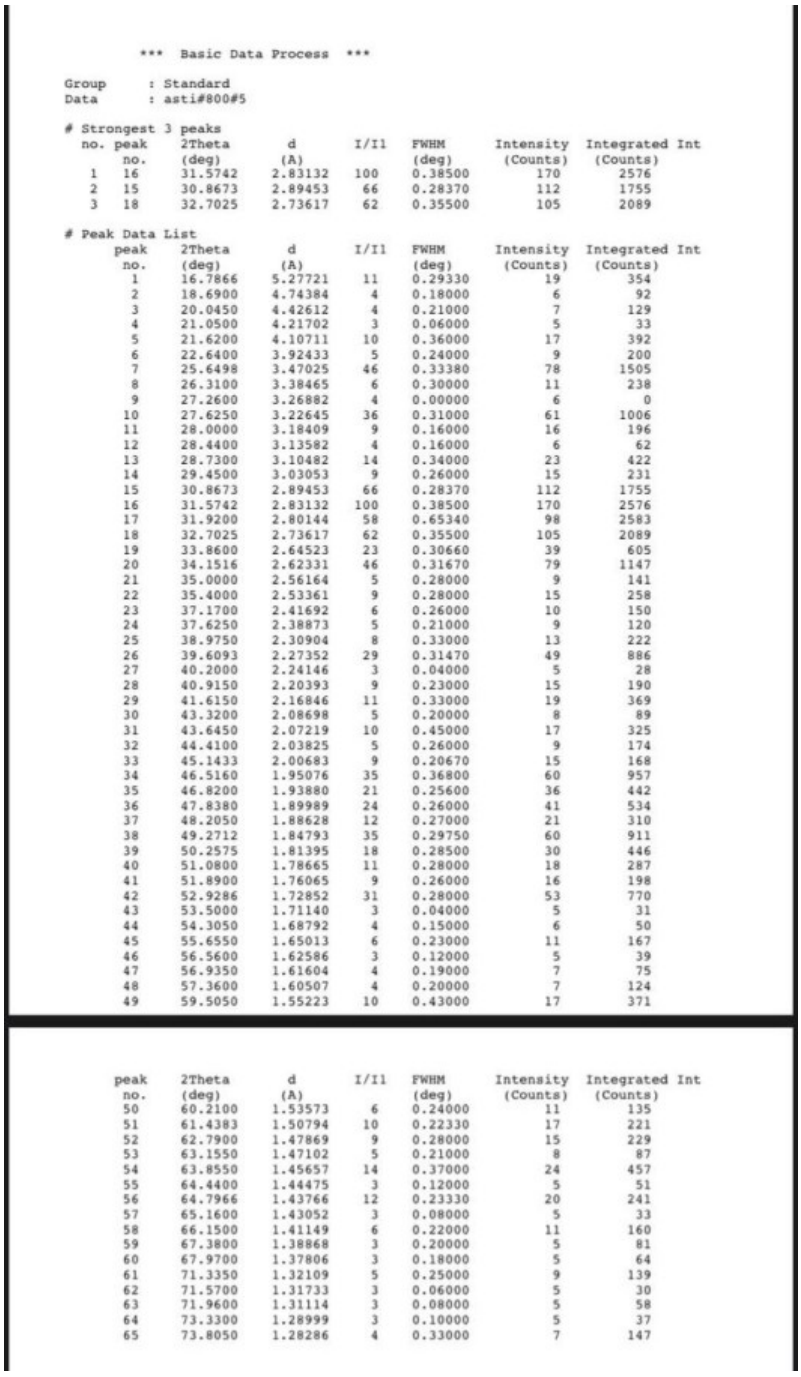

*** Basic Data Process ***

Group : Standard
Data : asti#800#5

Strongest 3 peaks

no.	peak no.	2Theta (deg)	d (A)	I/I1	FWHM (deg)	Intensity (Counts)	Integrated Int (Counts)
1	16	31.5742	2.83132	100	0.38500	170	2576
2	15	30.8673	2.89453	66	0.28370	112	1755
3	18	32.7025	2.73617	62	0.35500	105	2089

Peak Data List

peak no.	2Theta (deg)	d (A)	I/I1	FWHM (deg)	Intensity (Counts)	Integrated Int (Counts)
1	16.7866	5.27721	11	0.29330	19	354
2	18.6900	4.74384	4	0.18000	6	92
3	20.0450	4.42612	4	0.21000	7	129
4	21.0500	4.21702	3	0.06000	5	33
5	21.6200	4.10711	10	0.36000	17	392
6	22.6400	3.92433	5	0.24000	9	200
7	25.6498	3.47025	46	0.33380	78	1505
8	26.3100	3.38465	6	0.30000	11	238
9	27.2600	3.26882	4	0.00000	6	0
10	27.6250	3.22645	36	0.31000	61	1006
11	28.0000	3.18409	9	0.16000	16	196
12	28.4400	3.13582	4	0.16000	6	62
13	28.7300	3.10482	14	0.34000	23	422
14	29.4500	3.03053	9	0.26000	15	231
15	30.8673	2.89453	66	0.28370	112	1755
16	31.5742	2.83132	100	0.38500	170	2576
17	31.9200	2.80144	58	0.65340	98	2583
18	32.7025	2.73617	62	0.35500	105	2089
19	33.8600	2.64523	23	0.30660	39	605
20	34.1516	2.62331	46	0.31670	79	1147
21	35.0000	2.56164	5	0.28000	9	141
22	35.4000	2.53361	9	0.28000	15	258
23	37.1700	2.41692	6	0.26000	10	150
24	37.6250	2.38873	5	0.21000	9	120
25	38.9750	2.30904	8	0.33000	13	222
26	39.6093	2.27352	29	0.31470	49	886
27	40.2000	2.24146	3	0.04000	5	28
28	40.9150	2.20393	9	0.23000	15	190
29	41.6150	2.16846	11	0.33000	19	369
30	43.3200	2.08698	5	0.20000	8	89
31	43.6450	2.07219	10	0.45000	17	325
32	44.4100	2.03825	5	0.26000	9	174
33	45.1433	2.00683	9	0.20670	15	168
34	46.5160	1.95076	35	0.36800	60	957
35	46.8200	1.93880	21	0.25600	36	442
36	47.8380	1.89989	24	0.26000	41	534
37	48.2050	1.88628	12	0.27000	21	310
38	49.2712	1.84793	35	0.29750	60	911
39	50.2575	1.81395	18	0.28500	30	446
40	51.0800	1.78665	11	0.28000	18	287
41	51.8900	1.76065	9	0.26000	16	198
42	52.9286	1.72852	31	0.28000	53	770
43	53.5000	1.71140	3	0.04000	5	31
44	54.3050	1.68792	4	0.15000	6	50
45	55.6550	1.65013	6	0.23000	11	167
46	56.5600	1.62586	3	0.12000	5	39
47	56.9350	1.61604	4	0.19000	7	75
48	57.3600	1.60507	4	0.20000	7	124
49	59.5050	1.55223	10	0.43000	17	371

peak no.	2Theta (deg)	d (A)	I/I1	FWHM (deg)	Intensity (Counts)	Integrated Int (Counts)
50	60.2100	1.53573	6	0.24000	11	135
51	61.4383	1.50794	10	0.22330	17	221
52	62.7900	1.47869	9	0.28000	15	229
53	63.1550	1.47102	5	0.21000	8	87
54	63.8550	1.45657	14	0.37000	24	457
55	64.4400	1.44475	3	0.12000	5	51
56	64.7966	1.43766	12	0.23330	20	241
57	65.1600	1.43052	3	0.08000	5	33
58	66.1500	1.41149	6	0.22000	11	160
59	67.3800	1.38868	3	0.20000	5	81
60	67.9700	1.37806	3	0.18000	5	64
61	71.3350	1.32109	5	0.25000	9	139
62	71.5700	1.31733	3	0.06000	5	30
63	71.9600	1.31114	3	0.08000	5	58
64	73.3300	1.28999	3	0.10000	5	37
65	73.8050	1.28286	4	0.33000	7	147

d. Suhu 850°C

*** Basic Data Process ***

Group : Standard
Data : asti#850#5

Strongest 3 peaks

no.	peak no.	2Theta (deg)	d (A)	I/I1	FWHM (deg)	Intensity (Counts)	Integrated Int (Counts)
1	7	31.7480	2.81622	100	0.25130	386	5156
2	9	32.8846	2.72143	66	0.24180	256	3292
3	8	32.1466	2.78220	51	0.27780	195	2934

Peak Data List

peak no.	2Theta (deg)	d (A)	I/I1	FWHM (deg)	Intensity (Counts)	Integrated Int (Counts)
1	21.7400	4.08471	6	0.28000	23	384
2	22.8483	3.88902	5	0.20330	21	286
3	25.8435	3.44468	34	0.24160	133	1747
4	26.1000	3.41141	4	0.12000	17	158
5	28.0975	3.17326	9	0.26500	33	504
6	28.9037	3.08655	15	0.23250	59	791
7	31.7480	2.81622	100	0.25130	386	5156
8	32.1466	2.78220	51	0.27780	195	2934
9	32.8846	2.72143	66	0.24180	256	3292
10	33.1800	2.69787	4	0.09000	15	188
11	34.0333	2.63216	24	0.25330	92	1312
12	35.4213	2.53213	5	0.22930	20	274
13	39.1750	2.29772	7	0.18340	27	280
14	39.7770	2.26432	26	0.25740	100	1418
15	41.9790	2.15049	8	0.22200	29	401
16	43.8375	2.06354	6	0.23500	24	384
17	45.2735	2.00136	6	0.19700	22	240
18	46.6747	1.94449	36	0.24000	138	1869
19	48.0600	1.89163	15	0.24000	58	815
20	48.5741	1.87280	5	0.20170	18	210
21	49.4538	1.84153	44	0.22760	171	2117
22	50.4749	1.80664	19	0.23870	75	971
23	51.2546	1.78098	16	0.23580	61	731
24	52.0561	1.75543	15	0.24110	59	768
25	53.1797	1.72095	21	0.24940	81	1085
26	55.8450	1.64497	9	0.19000	35	434
27	57.1050	1.61163	5	0.25000	18	262
28	58.0416	1.58783	3	0.17670	13	206
29	59.9116	1.54266	6	0.24330	24	306
30	60.3800	1.53181	4	0.24000	16	220
31	61.6160	1.50401	10	0.21600	40	503
32	62.9575	1.47516	11	0.20500	43	518
33	64.0267	1.45308	12	0.32000	48	808
34	64.9945	1.43376	11	0.21760	41	518
35	66.3833	1.40709	5	0.19330	18	208
36	69.6733	1.34847	3	0.22670	12	158
37	71.5580	1.31752	5	0.19600	21	225
38	72.2075	1.30726	4	0.16500	15	149
39	73.9475	1.28074	6	0.25500	25	405

*** Basic Data Process ***

Data Infomation

Group : Standard
Data : asti#850#5
Sample Nmae : powder
Comment :
Date & Time : 01-12-24 07:52:15

Measurement Condition

X-ray tube
target : Cu
voltage : 40.0 (kV)
current : 30.0 (mA)
Slits
Auto Slit : not Used
divergence slit : 1.00000 (deg)
scatter slit : 1.00000 (deg)
receiving slit : 0.30000(mm)
Scanning

2. Analisis Data *X-Ray Diffraction* (XRD) dengan metode Debye-Scherrer

Tabel 1. Analisis Data XRD untuk ukuran kristal HAp pada suhu Suhu 700°C

Sudut Difraksi (2θ)	FWHM	K	λ	D (nm)
31.7794	0.7878	0.9	0.15405	10.48408095
32.7412	0.4825	0.9	0.15405	17.15944473
25.7183	0.4433	0.9	0.15405	18.38061682
RATA-RATA				**15.34138083**

Tabel 2. Analisis Data XRD untuk ukuran kristal HAp pada suhu Suhu 750°C

Sudut Difraksi (2θ)	FWHM	K	λ	D (nm)
31.5962	0.3476	0.9	0.15405	23.7503234
32	0.336	0.9	0.15405	24.59494921
32.7167	0.34	0.9	0.15405	24.34974207
RATA-RATA				**24.23167156**

Tabel 3. Analisis Data XRD untuk ukuran kristal HAp pada suhu Suhu 800°C

Sudut Difraksi (2θ)	FWHM	K	λ	D (nm)
31.5742	0.3476	0.9	0.15405	21.4419848
30.8673	0.2873	0.9	0.15405	29.0481068
32.7025	0.355	0.9	0.15405	23.32003168
RATA-RATA				**24.60337443**

Tabel 4. Analisis Data XRD untuk ukuran kristal HAp pada suhu Suhu 850°C

Sudut Difraksi (2θ)	FWHM	K	λ	D (nm)
31.748	0.2513	0.9	0.15405	32.86396768
32.8846	0.2418	0.9	0.15405	34.25344618
32.1466	0.2778	0.9	0.15405	29.75861178
RATA-RATA				**32.29200855**